JACS
JOURNAL OF THE AMERICAN CHEMICAL SOCIETY
Article
pubs.acs.org/JACS

Phosphorus-Containing Chiral Molecule for Fullerene Recognition Based on Concave/Convex Interaction

Masaki Yamamura,* Tsuyoshi Saito, and Tatsuya Nabeshima*

Graduate School of Pure and Applied Sciences and Tsukuba Research Center for Interdisciplinary Materials Science (TIMS), University of Tsukuba, 1-1-1, Tennodai, Tsukuba, Ibaraki 305-8571, Japan

Supporting Information

ABSTRACT: A C_3-symmetric chiral concave molecule having a phosphorus atom at the center was synthesized, and its enantiomers were resolved. The chiral concave shape and absolute structure of the concave molecules were revealed by X-ray analysis. The concave molecule exhibited intense chiroptical properties with a large anisotropy, which was derived from molecular orbitals delocalized to the side chains. In the co-crystal with pristine C_{60}, four of the enantiopure concave molecules perfectly wrapped the surface of C_{60}. MALDI-TOF mass, NMR, and circular dichromism spectra also supported the concave/convex interaction between the concave molecule and fullerene. These results suggest that the phosphorus-containing molecule with a concave shape plays an important role as a chiral host molecule for C_{60}.

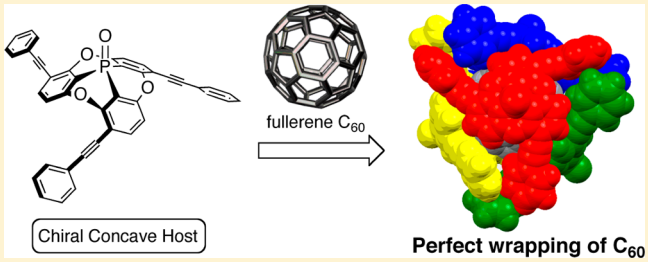

INTRODUCTION

The recognition of fullerenes (C_{60} and its higher analogues) is one of the most intensive research subjects in supramolecular and host–guest chemistry.[1] The applications for recognition of fullerene C_{60} include fullerene purification, nanoscale organization, and perturbation of its electronic and photonic properties. From a fundamental point of view, recognition of fullerene C_{60} is challenging as it involves capture of the spherical surface of fullerene, which has no functional groups. Thus, the driving force for C_{60} recognition is restricted to weak $\pi-\pi$, van der Waals and charge-transfer interactions, metal–π coordination, or the solvophobic effect. Design of host molecules whose size fits to guest C_{60} is important, as this can provide an enhancement of the weak interactions. In order to match with the "convex" surface of fullerenes, "concave-shaped" host molecules have been developed. Since the discovery of the selective formation of the C_{60}/calix[8]arene host–guest complex,[2] convex/concave-type recognition of fullerenes, mainly C_{60} and C_{70}, has emerged in a variety of concave host molecules, such as calix[4]arenes,[3] calix[5]-arenes,[4] homooxacalix[3]arene,[5] γ-cyclodextrin,[6] cyclotriveratrylene (CTV),[7] and so on.[8] Bowl-type π-conjugated molecules, for example, corannulene[9] and sumanene,[10] are promising host molecules because their concave surfaces closely resemble fullerene segments and can fit precisely to the convex surface of C_{60} (Chart 1). Recently, the interaction of corannulene with pristine C_{60} has been observed in a crystal structure, though it is not effective in solution.[11] In particular, these molecules are attractive because of their potential to function as chiral hosts based on "bowl-chirality".[12,13] It is expected that bowl-chirality combined with fullerene recognition could find application in asymmetric recognition of chiral fullerenes or asymmetric synthesis in fullerene derivatization. However, adequate synthetic methods for homochiral bowl-type hosts have not been sufficiently explored.[14] Efforts to develop bowl-type molecules are still required for improvement of fullerene recognition.

Chart 1. Concave Molecules

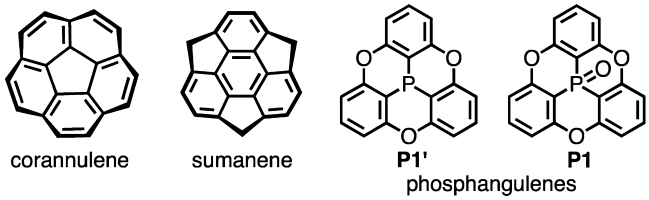

We envision a strategy for the design of a chiral concave molecule using a phosphorus-doping method, which can play a crucial role in construction of the concave structure. Generally, phosphorus atoms rarely adopt the s/p orbital hybridization observed in the second-row elements, C, N, and O, because its s and p orbitals are spatially and energetically separated.[15] Planar tertiary phosphine compounds have not been reported due to the difficulty in forming sp^2 hybrid orbital. Hence, phosphorus-doping into a planar π-conjugated system should lead to a concave surface due to the nonplanar phosphorus atom. Krebs and his colleagues reported the phosphorus-containing concave molecules, phosphangulenes **P1′** and **P1** (Chart 1).[16] These molecules are ideal candidates for chiral concave hosts because the phosphorus atom should prevent racemization based on bowl-inversion, which is frequently

Received: August 10, 2014
Published: September 11, 2014

   dx.doi.org/10.1021/ja507913u | J. Am. Chem. Soc. 2014, 136, 14299–14306

observed in bowl-type molecules composed of second-row elements. We now report the synthesis of the chiral concave molecule **P2** by extension of the π-surface of **P1**, the encapsulation of the C_{60} convex surface by **P2**, and the induction of chiroptical properties of C_{60} by **P2**.

RESULTS AND DISCUSSION

Synthesis and Chiral Resolution. The brominated derivative **P3** was chosen as a precursor for the π-extended concave molecules (Scheme 1). However, the bromination of

Scheme 1

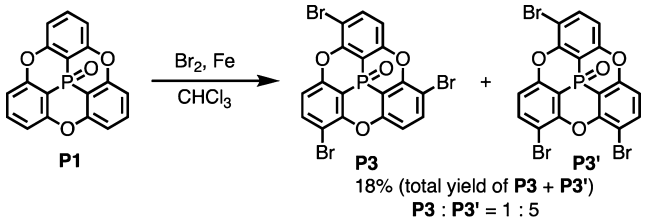

P1 gave the tribrominated compound in low yield together with dibrominated and tetrabrominated products. The mole ratio of the two isomers of tribromides, the targeted C_3-symmetric **P3** and C_1-symmetric **P3′**, was 1:5 as determined by ^{1}H NMR. The products ratio is close to the statistical value (1:3), indicating no selectivity of the reaction. This result forced us to reconsider the synthetic strategy.

Since the selective bromination of highly symmetric **P1** is difficult, the less symmetric precursor was brominated before the bowl-shape formation (Scheme 2). Brominated compound

Scheme 2

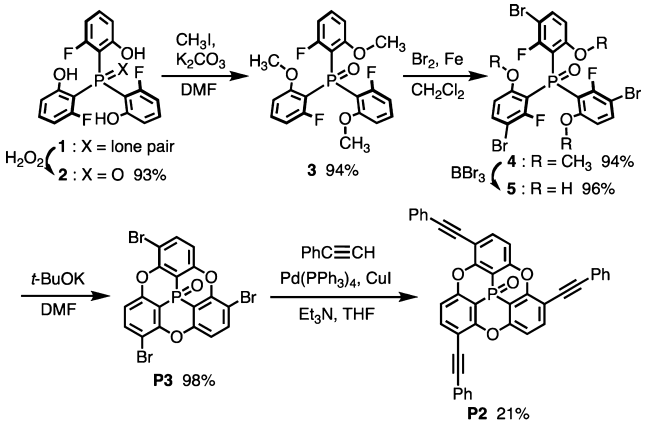

5 was synthesized from known compound **1**[16a] in four steps in 79% overall yield. Intramolecular S_NAr reactions in **5** gave **P3** in 98% yield. The Sonogashira coupling reaction of **P3** gave concave compound **P2** as a racemic mixture in 21% yield.

The enantiomers of **P2** were well resolved by preparative chiral HPLC (Figure 1). The optical density (OD) values of the two peaks are almost the same. The optical rotation (OR) signal of one enantiomer is the mirror image of the other. The absolute structures of the enantiomers were determined by X-ray analysis and circular dichromism (CD) spectra, described below.

Crystallization of a racemic mixture *rac*-**P2** from hexane/chloroform gave a single crystal suitable for X-ray crystallographic analysis with the centrosymmetric space group *C*2/*c*.

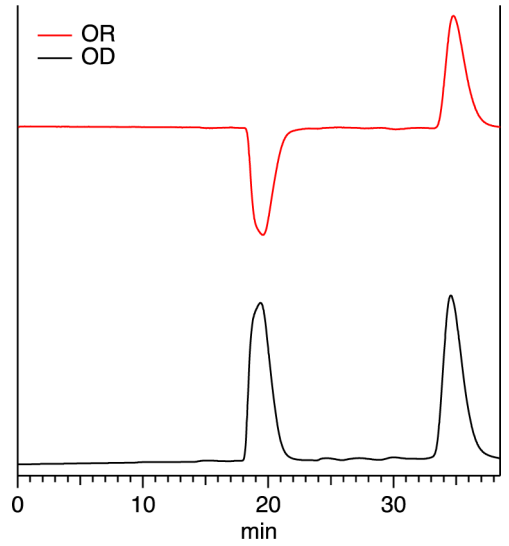

Figure 1. Chiral HPLC profiles of *rac*-**P2** (Daicel Chiralpak IA, eluent 1:1 hexane/chloroform; OR and OD values at 300 nm).

Both enantiomers are present in the unit cell. One of the enantiomers, *M*-**P2**,[12] is shown in Figure 2. Although there are

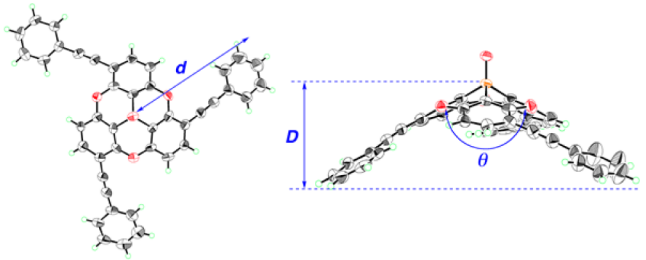

Figure 2. ORTEP drawing of *rac*-**P2** with 50% thermal ellipsoid, top (left) and side (right) views. Only the *M*-isomer is shown.

four independent molecules in the unit cell, the structures of all the molecules are very similar to each other. The three side chains, phenylacetylene groups, are arranged in a right-hand-turning propeller fashion. The torsion angles of the three phenyl groups in the phosphangulene unit are 50.1−51.6°, which clearly reveals the curved structure of **P2**. The torsion angles between the two phenyl groups in the diphenylacetylene units are 8.8−47.5° (mean 23.7°) because the terminal phenyl groups freely rotate. The distance from the central phosphorus atom to the edge of the side chain, *d*, is 11.2 Å. Bond angles C−P−C are 97.4(2)−99.2(2)°, enforcing the distorted surface. The bowl depth of **P2**, *D*, is 3.91 Å, and the bowl cone angle, θ, is 121.6°. The total area of the concave surface is calculated from these parameters to be 324 Å^2, which is similar to the calculated CPK area, 308 Å^2. As we discuss later, four convex surfaces of **P2** perfectly encapsulate C_{60}. Recrystallization of enantiopure *M*-**P2** from methanol/chloroform gave a single crystal with the chiral space group $P2_1$. X-ray analysis revealed that the fraction showing positive OR signal in the chiral HPLC is assigned to the absolute structure of *M*-**P2**, with a Flack χ value of −0.12(14). The crystal structure of enantiopure *M*-**P2** is very similar to that of the racemic one.

Chiroptical Properties and Electronic Structures. The UV−vis absorption and CD spectra of **P2** were measured in chloroform (Figure 3). The absorption maximum of **P2** is 300

dx.doi.org/10.1021/ja507913u | J. Am. Chem. Soc. 2014, 136, 14299−14306

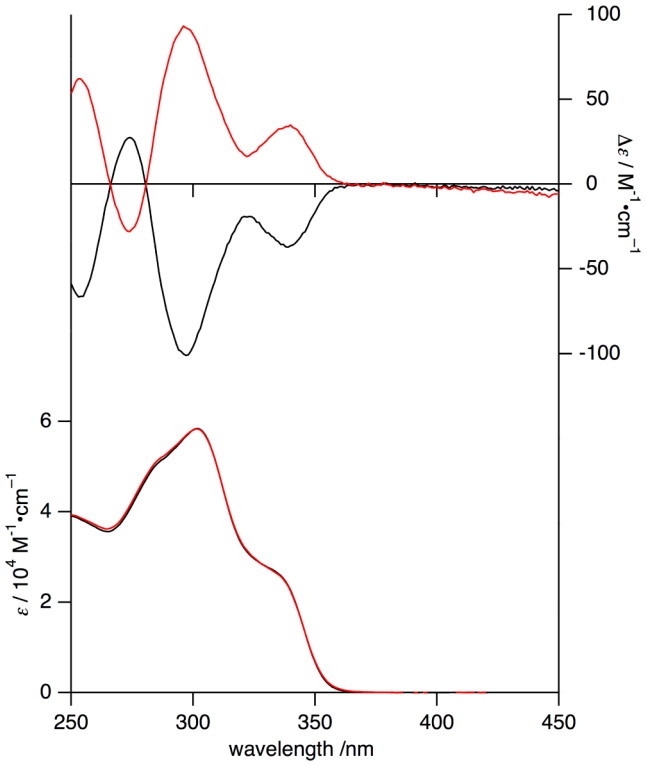

Figure 3. UV−vis absorption (bottom) and CD (top) spectra of *M*- (red) and *P*-**P2** (black) in chloroform.

nm, with a shoulder at ca. 330 nm. The molar extinction coefficient, ε, of **P2** is larger than that of **P1** without any side groups, reflecting the elongated π-conjugation in **P2**. The CD spectra of the two enantiomers of **P2** are complete mirror images. *M*- and *P*-**P2** show positive and negative Cotton effects, respectively, in the range of 300−350 nm. The anisotropy factor of absorbance, $g_{abs} = (I_+ - I_-)/(I_+ + I_-) = 2\Delta\varepsilon/\varepsilon$ at θ_{max}, for *M*-**P2** was determined by using ε and setting the molar circular dichromism, $\Delta\varepsilon$, to a large value of $+3.6 \times 10^{-3}$ (Table 1). The specific rotation, $[\alpha]_D$, of *M*-**P2** is also a large value,

Table 1. Spectroscopic and Photophysical Data of *M*-P2 and P1

		M-P2	P1
Abs	λ_{abs}/nm	300	305
	ε/cm^{-1}·M^{-1}	5.84×10^4	9.69×10^3
CD	λ_{CD}/nm	297	–
	$\Delta\varepsilon$/cm^{-1}·M^{-1}	+101	–
	g_{abs}	$+3.6 \times 10^{-3}$	–
FL	λ_{flu}/nm	363	332
	Φ_{flu}[a]	14%	2%

[a]Quantum yields were determined by the absolute method using an integrating sphere instrument.[20]

+1122 (*c* 0.068, chloroform). Both g_{abs} and $[\alpha]_D$ for *M*-**P2** are half as large as those values for helicene[5], $+8.3 \times 10^{-3}$ and +2760,[17] respectively, which is well known as a compound that shows an exceptionally strong Cotton effect.

P2 shows fluorescence at 363 nm, which is red-shifted from that of **P1** (λ_{flu} = 332 nm) (Figure 4). In addition, the absolute fluorescence quantum yield, Φ_{flu}, of **P2**, 14%, is much higher than that of **P1**, 2%.

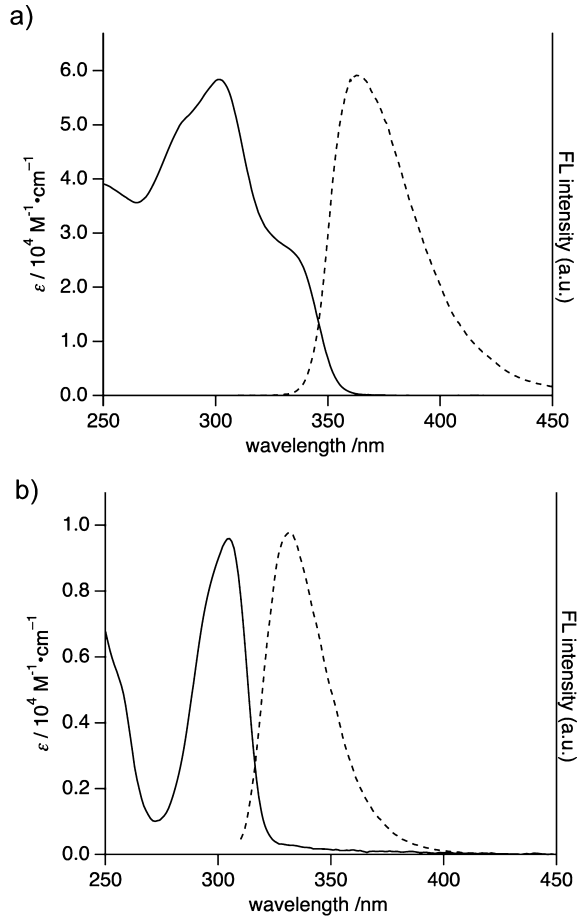

Figure 4. UV−vis absorption and fluorescence spectra of (a) *rac*-**P2** and (b) **P1** in chloroform.

A time-dependent (TD)-DFT calculation was performed on the structurally optimized *M*-**P2** at the M06-2X/6-311+G-(2d,p)//M06-2X/6-31G(d,p) level in order to clarify the details of the electronic structure. The Kohn−Sham molecular orbitals (MOs) of *M*-**P2** are shown in Figure 5. The MOs are categorized into C_3-symmetric *a* orbitals and doublet *e* orbitals, an irreducible representation of the C_3 point group.[18] The HOMO and HOMO−1 are doublet *e* orbitals, and the HOMO−2 is an *a* orbital. These three orbitals are linear combinations of the π-orbitals of the three diphenylacetylene side-chain units. On the other hand, the LUMO is an *a* orbital, and the LUMO+1 and LUMO+2 are doublet *e* orbitals, which are basically π^*-orbitals of the diphenylacetylene units. The LUMO is a π^*-orbital with a contribution from a phosphorus-centered p_z-orbital in an antibonding P−O orbital, i.e., the $\pi^*-\sigma^*$ conjugated orbital.[19] The conjugation with the phosphorus-centered p_z-orbital should stabilize the LUMO orbital. The phosphorus-centered p_z-orbital does not participate in the LUMO+1 and LUMO+2 because the combination is symmetry-forbidden.

The singlet excitation energies of *M*-**P2** are lower than those of **P1** (Table 2). It is difficult to resolve the spectroscopic properties into the component orbitals because most of the excitation states consist of several transitions. However, the excited states are categorized into *A* and doublet *E* wave functions, which provide helpful interpretations of the spectroscopic properties based on point group symmetry. The *E* states of C_{3v}-symmetric **P1** are electrically and

dx.doi.org/10.1021/ja507913u | J. Am. Chem. Soc. 2014, 136, 14299−14306

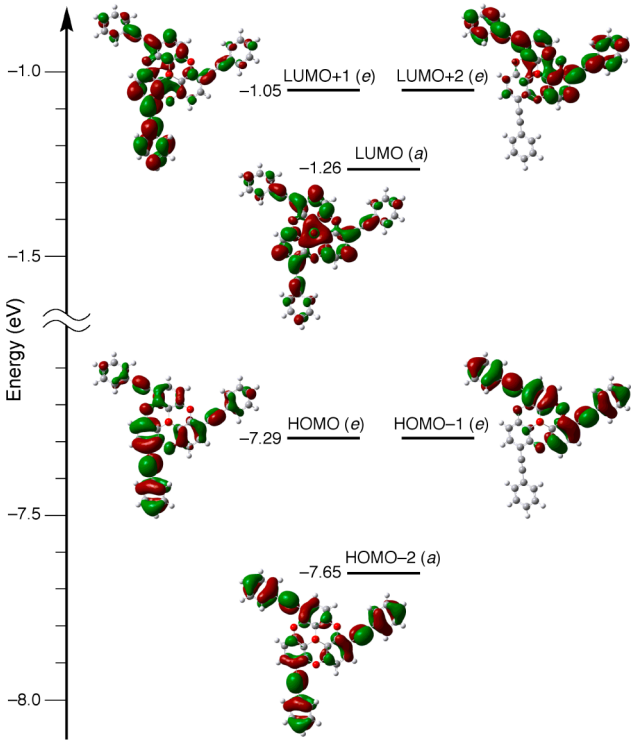

Figure 5. Kohn−Sham orbitals of *M*-**P2** (M06-2X/6-311+G(2d,p)//M06-2X/6-31G(d,p)).

magnetically allowed, while the *A* excited states are forbidden excitations. The calculated oscillator strengths, *f*, of the S_1 and S_2 states (*E*) of *M*-**P2**, which is related to $|\mu_e|^2$ (where μ_e is the electric dipole transition moment), are much larger than those of those of **P1**. These results are consistent with the experimental absorption and fluorescence spectra. The extension of π-conjugation significantly affects the optical properties.

The calculated rotational strengths, *R*, of the S_1 and S_2 states (*E*) of *M*-**P2**, which is related to $\mathrm{Im}(\mu_e \cdot \mu_m)$ (where μ_m is the magnetic dipole transition moment),[21] are significantly large, positive values, as shown in the experimental CD spectra. The μ_e and μ_m of the *E* states of **P1** and *M*-**P2** are illustrated in Figure 6. In **P1**, the μ_m is precisely vertical to the μ_e ($\mu_e \cdot \mu_m$ = 0). The bowl structure of **P1** is necessary to the allowed μ_m value because the planar D_{3h}-symmetric compounds are magnetically forbidden. The wave function of *M*-**P2** is divided into two parts, the core part similar to **P1** and the side-chain phenylacetylenes part. The core unit should have μ_e(core) and μ_m(core) similar to thosse of **P1**. The μ_e(side) and μ_m(side) in the side part are rotated anticlockwise around the P−O bond axis. The μ_e and μ_m in each part are vertical. However, μ_e(tot) and μ_m(tot) in the whole molecule are no longer vertical. As a result, the rotatory strength is not zero. In summary, the CD signals of *M*-**P2** originate from the anisotropic orientation of the core and side parts.

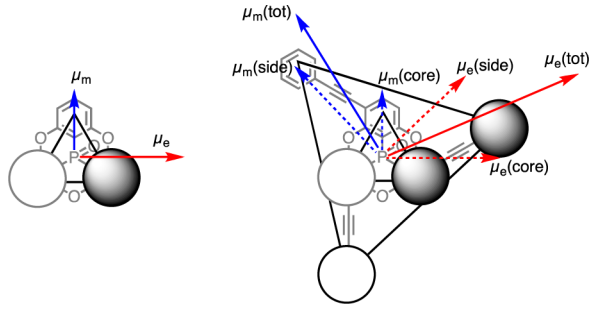

Figure 6. Calculated μ_e and μ_m of the *E* excited states of **P1** and *M*-**P2**.

Fullerene Encapsulation and Induction of Chiroptical Properties. In the previous section, the remarkably intense chiroptical property of **P2** was confirmed on the basis of its bowl-chirality. The next challenge is the application of **P2** as a concave chiral host for inducing the chiroptical property to a convex guest, fullerene. Among many studies of fullerene encapsulation, X-ray analysis has been a very powerful tool to observe the concave/convex adducts.[22] Even if the interaction is weak, the encapsulation complex should be maintained in the crystal.[8a,b,o,14] Co-crystals of pristine C_{60} with *P*-**P2** were isolated as black crystals by allowing their toluene solution to stand. Single crystals suitable for X-ray diffraction measurements were obtained by recrystallization from dichloromethane/CS_2. The space group of the co-crystal is non-centrosymmetric $I4_1$, with Flack χ value of −0.01(3). The central C_{60} was encapsulated by a chiral cavity surrounded by four *P*-**P2** molecules (Figure 7a). Although two of the four *P*-**P2** molecules are crystallographically independent, only the orientation of the side phenyl groups was different in the two independent molecules. Almost the entire surface of C_{60} was covered with the *P*-**P2** molecules. The phosphorus-containing unit of *P*-**P2** made contact with the C_{60} surface in a concave/convex way. The phenylacetylene side chains of three *P*-**P2** molecules made contact with each other and were arranged in pseudo-C_3-symmetry (Figure 7a, right).

It is noteworthy that the C_{60} was not disordered at all and was represented with small temperature factors (Figure 7b). The C−C bond lengths of the C6 rings of the C_{60} range from 1.375(5) to 1.395(5) Å. The C−C bond lengths that join the C6 and C5 rings range from 1.440(4) to 1.469(5) Å. These structural parameters are well comparable with those of C_{60} (C6−C6 bond 1.38 Å and C6−C5 bond 1.45 Å).[1a,23] Often, highly symmetric guest C_{60} molecules are disordered in the crystal cavity.[24] However, when interactions with the cavity are

Table 2. Singlet Electronic Excitation of *M*-P2 and P1 Based on TD-DFT

	excited state	wave function[a]	λ/nm	*f*	*R*[b]
M-**P2**	S_1 (*E*)	0.50H−1 → L	297	1.267	541.23
	S_2 (*E*)	0.50H → L	297	1.267	541.08
	S_3 (*E*)	0.42H → L+3	279	0.329	198.17
P1	S_1 (*E*)	0.60H → L	260	0.0830	−0.044
	S_2 (*E*)	0.60H−1 → L	260	0.0829	−0.058
	S_3 (*A*)	0.32H−1 → L+2 + 0.32H → L+1	242	0.0000	0.126

[a]The sum of the squares of the expansion coefficients is normalized to total 1/2. [b]10^{-40} cgs (velocity).

dx.doi.org/10.1021/ja507913u | J. Am. Chem. Soc. 2014, 136, 14299−14306

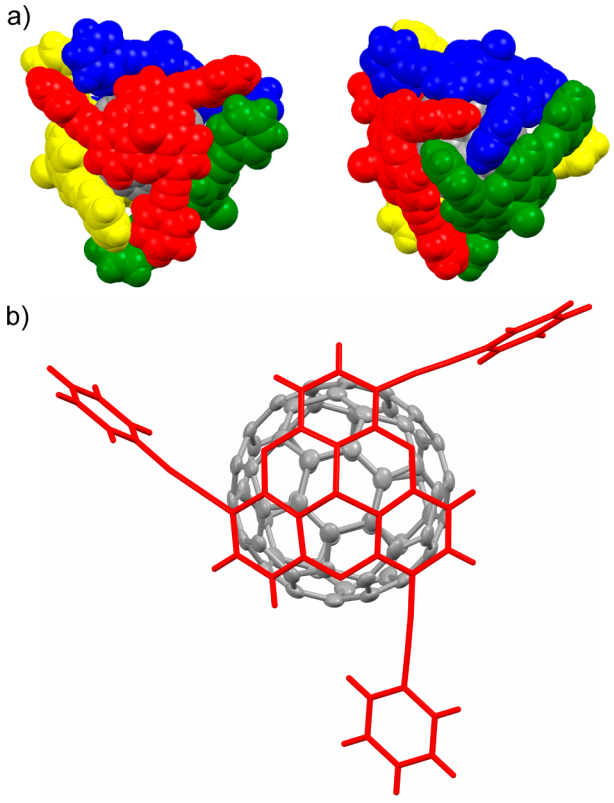

Figure 7. (a) Space-filling representation of the crystal structure of (*P*-**P2**)$_4$⊃C_{60}, top (left) and side (right) views. The four *P*-**P2** molecules are colored red, green, blue, and yellow. The central C_{60} molecule is colored gray. The red and blue molecules are crystallographically equivalent, as are the yellow and green ones. (b) ORTEP drawing of the C_{60} part in (*P*-**P2**)$_4$⊃C_{60} with 50% thermal ellipsoids. One *P*-**P2** molecule is drawn with capped-sticks representation to clarify the C_{60} orientation.

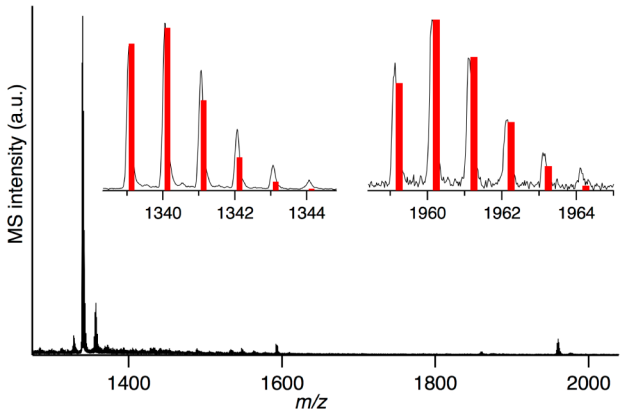

Figure 8. MALDI-TOF MS of (*P*-**P2**)$_4$⊃C_{60} (negative). The black line shows the observed spectrum, and red bars show the simulated isotope peak clusters for [(*P*-**P2**)$_2$⊃C_{60}−H]$^-$ and [*P*-**P2**⊃C_{60}−H]$^-$.

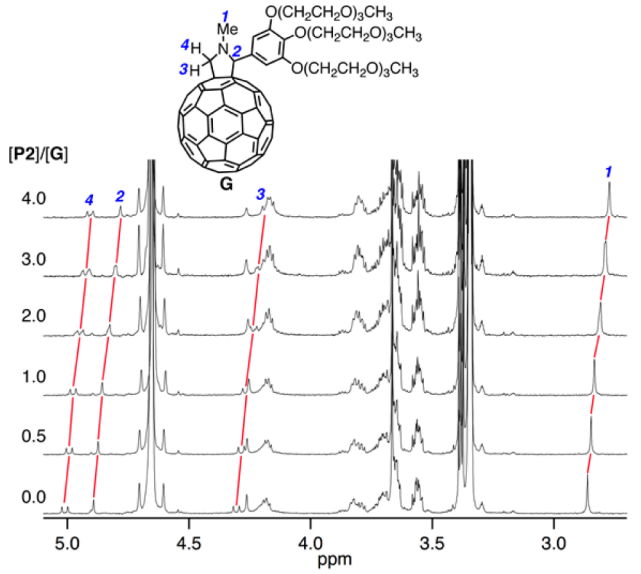

Figure 9. ^{1}H NMR titration (600 MHz, 1:1 $CDCl_3/CD_3OD$ (v/v), 1 mM) of **G** with addition of *rac*-**P2**, 0 ≤ [**P2**]/[**G**] ≤ 4.

strong, the orientation of guest C_{60} should be fixed within the crystal. A 3-fold rotation axis in the center of a six-membered ring of C_{60} matches up almost precisely with the 3-fold pseudo-rotation axis of *P*-**P2**. In addition, the centroid of the three side chains is located on the 3-fold rotation axis of C_{60}, which suggests the involvement of the side chains in the interaction with C_{60}.

A MALDI-TOF mass spectrum of (*P*-**P2**)$_4$⊃C_{60} shows prominent peaks at m/z = 1959.1 and 1339.0 (Figure 8), which correspond to [(*P*-**P2**)$_2$⊃C_{60}−H]$^-$ and [*P*-**P2**⊃C_{60}−H]$^-$, respectively. Although the parent molecular ion itself was not observed, this result revealed that the concave/convex interaction is strong enough to maintain the encapsulated complex even during ionization.

^{1}H NMR spectroscopic titration was carried out to evaluate the quantitative concave/convex interaction.[25] The change of the ^{1}H NMR signals of *rac*-**P2** was negligible upon the addition of C_{60} in a good solvent, 1:1 $CDCl_3/CS_2$. This suggests that the interaction with C_{60} is very weak in the solvent. Thus, a more polar solvent was chosen because the solvophobic effect should support the formation of the host−guest complex.[26] The C_{60} derivative **G**, having soluble triethylene glycol chains,[27] was used instead of pristine C_{60}, which is insoluble in polar media (Figure 9). The ^{1}H NMR signals of the pyrrolidine units of **G** shifted upfield upon the addition of **P2** in 1:1 $CDCl_3/CD_3OD$, which suggests host−guest interactions in the solution. The Job's plot indicated 1:1 association of **P2** with **G**, though a 4:1 complex was formed in the crystal. The interaction is likely to be too weak to form higher host−guest complexes such as 2:1 and 3:1. Nonlinear least-squares analysis of the chemical-shift change afforded the association constant, K_a, of 183 ± 26 M^{-1}.[28] In contrast, a chemical-shift change was not observed upon addition of **P1** to **G**. These results reveal that the side phenylacetylene chains play an important role in the interaction with fullerene.

The chemical shifts of **P2** also changed by the interaction with **G** (Figure 10). The protons *a* and *b* on the phosphorus-containing unit were shifted upfield upon the addition of **G**, while the protons on the side Ph groups hardly changed at all. This is consistent with the host−guest complex having the same concave/convex interaction observed in the crystal structure, as only the *a* and *b* protons should be present in the shielded region of the fullerene.

Chirality induction to guest **G** from host molecule **P2** was observed in the CD spectra. Guest molecule **G** showed absorption in the 400−700 nm region, where host **P2** is transparent. An induced CD (ICD) signal of **G** was definitely observed between 400 and 500 nm upon the addition of *M*-**P2**

dx.doi.org/10.1021/ja507913u | J. Am. Chem. Soc. 2014, 136, 14299−14306

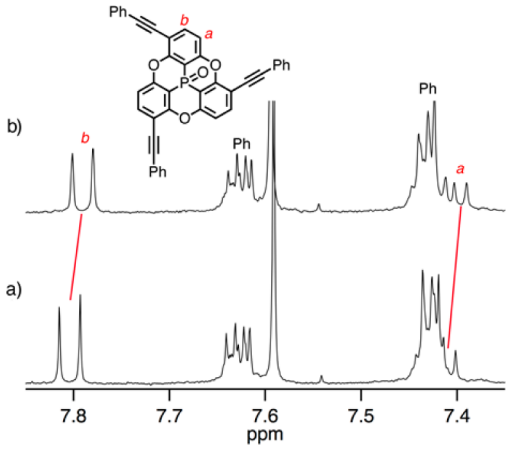

Figure 10. ^{1}H NMR spectra (600 MHz, 1:1 $CDCl_3/CD_3OD$ (v/v), 1 mM) of *rac*-**P2**, (a) without and (b) with 1.0 equiv of **G**.

or *P*-**P2**. The sign of the signals is the same as that of *M*-**P2** or *P*-**P2** in the UV region (~300 nm). In the absence of **G**, no CD signal was observed at 400−500 nm. Although the signal intensity is low, the mirror-image spectra for the enantiomers confirmed that the signals were definitely assigned to the host-induced CD of the guest. To the best of our knowledge, there have been few reports describing the transfer of the chiroptical properties from a chiral host to an achiral guest fullerene.[29,30] The concave host **P2**, having the bowl-type chirality, is expected to be an efficient chiral host for various fullerenes.

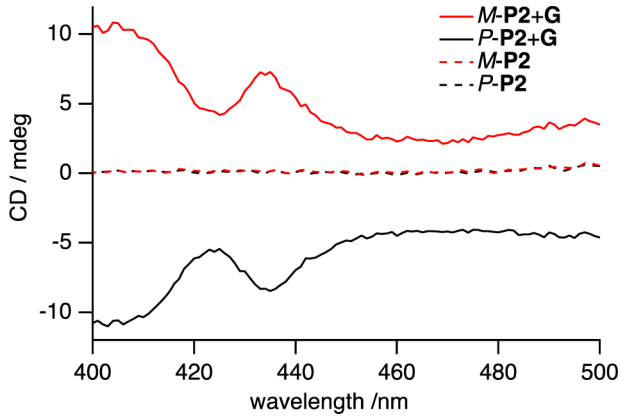

Figure 11. CD spectra of *M*-**P2** and *P*-**P2** in the presence or absence of **G** in 1:1 chloroform/methanol (v/v). [**G**] = 0.33 mM, [**P2**] = 4.0 mM.

CONCLUSION

We synthesized the C_3-symmetric chiral concave molecule **P2** having a phosphorus atom at the center and resolved the enantiomers. The chiral concave structure was revealed by X-ray analysis. The concave molecule **P2** exhibited chiroptical properties with a large anisotropy, the details of which were confirmed by TD-DFT calculation. In the co-crystal with C_{60}, four molecules of enantiopure **P2** perfectly wrapped the surface of C_{60}. MALDI-TOF mass and NMR spectra also supported the concave/convex interaction between **P2** and guest fullerene. Furthermore, the observation of the ICD signal of the guest fullerene indicates the transfer of the chiroptical properties of **P2** to the guest. These results suggest that **P2** is a component of a chiral assembled host $(P\text{-}\mathbf{P2})_4$ for C_{60}. The self-assembly of **P2** would lead to efficient encapsulation of fullerenes due to cooperative recognition, resulting in asymmetric recognition of chiral fullerenes like C_{76}.[31] This topic is now under investigation.

EXPERIMENTAL SECTION

General Methods. Compounds **P1** and **1** were synthesized according to Krebs's procedure.[16a] Full synthetic details for **1**−**5** are provided in the Supporting Information. An enantiomeric mixture of **P2** was separated by preparative HPLC using a Daicel Chiralpak IA column. Melting points were determined using a Yanaco melting point apparatus and are uncorrected. The ^{1}H, ^{13}C, and ^{31}P NMR spectra were recorded on Bruker DPX300 (300 MHz), AVANCE400 (400 MHz), or AVANCE600 (600 MHz) spectrometers. In the NMR measurements, tetramethylsilane was used as the internal standard (0 ppm) for ^{1}H and ^{13}C NMR, and phosphorous acid was used as the external standard (0 ppm) for ^{31}P NMR. The IR spectra were recorded on a JASCO FT/IR-480Plus spectrometer. MALDI-TOF mass spectra were recorded on an AB Sciex TOF/TOF5800 instrument. UV−vis absorption spectra were recorded an a JASCO Ubest V-660 spectrometer. Circular dichlomism spectra were recorded on a JASCO J-820W instrument. Specific rotation ($[\alpha]_D$) was measured at 21.0 °C in chloroform using a JASCO DIP-1000 polarimeter. Fluorescence spectra were recorded on a JASCO FP-8600 spectrometer. Absolute quantum yields were measured using Hamamatsu Photonics C9920-02 absolute photoluminescence quantum yield measurement system.

Synthesis of *rac*-P3 (Tribromophosphangulene). To a DMF (60 mL) solution of **5** (1.507 g, 2.443 mmol) was added *t*-BuOK (823 mg, 7.33 mmol), and the mixture was stirred at 140 °C for 23 h. After evaporation, distilled water (100 mL) was added. The mixture was extracted with chloroform. The combined organic phase was dried over $MgSO_4$, and then evaporation gave a crude brown powder. The crude products were washed with hexane to give a pale brown powder of *rac*-**P3** (1.327 g, 98%): ^{1}H NMR (400 MHz, $CDCl_3$) δ 7.24 (dd, J_{H-H} = 8.8, J_{H-P} = 5.2 Hz, 3H), 7.73 (d, J_{H-H} = 8.8 Hz, 3H); ^{31}P NMR (162 MHz, $CDCl_3$) δ −48.1 (s); ^{13}C NMR (100 MHz, $CDCl_3$) δ 107.9 (*C*, d, J_{C-P} = 7.3 Hz), 110.8 (*C*, d, J_{C-P} = 106 Hz), 117.1 (CH, d, J_{C-P} = 5.5 Hz), 137.0 (CH), 155.6 (*C*), 158.6 (*C*); MALDI-TOF MS *m*/*z* 556.77 $[M+H]^+$. Anal. Calcd for $C_{18}H_6O_4PBr_3$: C, 33.08; H, 1.26. Found: C, 33.25; H, 1.43.

Synthesis of *rac*-P2 (Tris(phenylethynyl)phosphangulene). To a THF/Et_3N (5 mL/10 mL) suspension of **P3** (202 mg, 0.363 mmol), CuI (40.4 mg, 0.212 mmol), and $Pd(PPh_3)_4$ (212 mg, 0.183 mmol) was added phenylacetylene (0.60 mL, 5.5 mmol), and the reaction mixture was stirred at 60 °C for 62 h. After evaporation of solvent, water (100 mL) and saturated NaCl (30 mL) were added. The mixture was extracted with chloroform. The organic phase was dried over $MgSO_4$, followed by evaporation. The crude products were separated by silica-gel column chromatography (chloroform/ethanol = 19:1) and preparative HPLC (GPC, chloroform) to give colorless prisms of *rac*-**P2** (46.6 mg, 21%): ^{1}H NMR (400 MHz, $CDCl_3$) δ 7.32 (dd, J_{H-H} = 8.7, J_{H-P} = 5.0 Hz, 3H), 7.38−7.42 (m, 9H), 7.61 (dd, *J* = 7.5 Hz, 4.3 Hz, 6H), 7.70 (d, J_{H-H} = 8.7 Hz, 3H); ^{31}P NMR (162 MHz, $CDCl_3$) δ −49.8 (s); ^{13}C NMR (100 MHz, $CDCl_3$) δ 82.2 (*C*), 95.7 (*C*), 109.8 (*C*, d, J_{C-P} = 108 Hz), 111.6 (*C*, d, J_{C-P} = 6.4 Hz), 115.7 (CH, d, J_{C-P} = 5.5 Hz), 122.7 (*C*), 128.5 (CH), 128.9 (CH), 131.8 (CH), 137.0 (CH), 158.9 (*C*), 159.0 (*C*); IR (KBr) ν 2208 cm^{-1} (C≡C), 1233 cm^{-1} (P═O); MALDI-TOF MS *m*/*z* 621.13 $[M+H]^+$. Anal. Calcd for $C_{42}H_{21}O_4P{\cdot}0.3H_2O$: C, 80.58; H, 3.48. Found: C, 80.46; H, 3.79.

X-ray Crystallography. X-ray diffraction measurements were performed using a Bruker APEXII ULTRA instrument. The X-ray diffraction intensities were collected on a CCD diffractometer at 120 K using Mo Kα (graphite-monochromated, λ = 0.71073 Å) radiation. The data were integrated with SAINT software (Bruker, 2004), and an empirical absorption correction (SADABS) was applied. The structure was solved by the direct method of the SIR-2004 program[32] and

dx.doi.org/10.1021/ja507913u | J. Am. Chem. Soc. 2014, 136, 14299−14306

refined using the SHELXL97 and SHELXL2014 programs.[33] All of the positional parameters and thermal parameters of non-hydrogen atoms were anisotropically refined on F^2 by the full-matrix least-squares method. Hydrogen atoms were placed at the calculated positions and refined riding on their corresponding carbon atoms. The crystallographic data for *rac*-**P2**, *M*-**P2**, and $(P\text{-}\mathbf{P2})_4\supset C_{60}$ were deposited with the Cambridge Crystallographic Data Center as supplementary publications CCDC 1016205, 1016206, and 1016207, respectively. Copies of the data can be obtained free of charge on application to CCDC, 12 Union Rd., Cambridge CB2 1EZ, U.K. (fax: (+44) 1223-336-033; email: deposit@ccdc.cam.ac.uk).

rac-**P2**: $C_{42}H_{21}O_4P\cdot CHCl_3$, MW 739.30, monoclinic, $C2/c$, a = 79.378(7), b = 12.2996(10), and c = 31.089(3) Å, β = 112.633(2)°, V = 28016(4) Å^3, Z = 32, D_{calc} = 1.403 Mg/m^3, μ = 0.352 mm^{-1}, no. reflections collected/unique = 77 431/31 674 [R_{int} = 0.0579], $R_1(I > 2\sigma(I))$ = 0.0928, wR_2 (all data) = 0.2144, goodness of fit (F^2) = 1.122, max. (min.) residual electron density = 0.962 (−0.908) e·Å^{-3}.

M-**P2**: $C_{42}H_{21}O_4P$, MW 620.56, monoclinic, $P2_1$, a = 11.548(3), b = 16.863(4), and c = 16.778(4) Å, β = 100.312(3)°, V = 3214.5(12) Å^3, Z = 4, D_{calc} = 1.282 Mg/m^3, μ = 0.129 mm^{-1}, no. reflections collected/unique = 33 120/12 583 [R_{int} = 0.0335], $R_1(I > 2\sigma(I))$ = 0.0885, wR_2 (all data) = 0.2634, goodness of fit (F^2) = 1.013, Flack χ = −0.12(14), max. (min.) residual electron density = 1.436 (−0.365) e·Å^{-3}.

$(P\text{-}\mathbf{P2})_4\supset C_{60}$: $C_{228}H_{84}O_{16}P_4$, MW 3202.84, tetragonal, $I4_1$, a = 31.285(6) and c = 16.399(4) Å, V = 16051(6) Å^3, Z = 4, D_{calc} = 1.325 Mg/m^3, μ = 0.120 mm^{-1}, no. reflections collected/unique = 70 886/18 284 [R_{int} = 0.0352], $R_1(I > 2\sigma(I))$ = 0.0569, wR_2 (all data) = 0.1399, goodness of fit (F^2) = 1.162, Flack χ = −0.01(3), max. (min.) residual electron density = 0.613 (−0.391) e·Å^{-3}.

Computational Methods. The DFT calculations were performed using the Gaussian09 packages[34] with the M06-2X functional.[35] The geometry optimizations of **P1** and **P2** were performed using the basis set 6-31G(d,p). Time-dependent calculations were performed at the equilibrium geometries using the basis set 6-311+G(2d,p).

■ ASSOCIATED CONTENT

Supporting Information

Detailed synthetic procedures, characterization data, calculation results, and crystallographic files (CIF). This material is available free of charge via the Internet at http://pubs.acs.org.

■ AUTHOR INFORMATION

Corresponding Authors

myama@chem.tsukuba.ac.jp
nabesima@chem.tsukuba.ac.jp

Notes

The authors declare no competing financial interest.

■ ACKNOWLEDGMENTS

We thank Prof. Dr. Hidetaka Yuge and Prof. Dr. Kazumasa Kajiyama (Kitasato University) for their assistance in chiral resolution using their preparative HPLC instrument. We also thank Prof. Dr. Mao Minoura (Rikkyo University) for his helpful discussion about X-ray crystallography. This research was financially supported by Grants-in-Aid for Scientific Research from the Ministry of Education, Culture, Sports, Science, and Technology of Japan.

■ REFERENCES

(1) (a) Martin, N., Nierengarten, J.-F., Eds. *Supramolecular Chemistry of Fullerenes and Carbon Nanotubes*; Wiley-VCH: Weinheim, 2012. (b) D'Souza, F., Kadish, K. M., Eds. *Handbook of Carbon Nano Materials, Vol. 1. Syntheses and Supramolecular Systems*; World Scientific Publishers: Singapore, 2011.

(2) (a) Atwood, J. L.; Koutsantonis, G. A.; Raston, C. L. *Nature* **1994**, *368*, 229. (b) Suzuki, T.; Nakashima, K.; Shinkai, S. *Chem. Lett.* **1994**, 699.

(3) (a) Barbour, L. J.; Orr, G. W.; Atwood, J. L. *Chem. Commun.* **1997**, 1439. (b) Georghiou, P. E.; Mizyed, S.; Chowdhury, S. *Tetrahedron Lett.* **1999**, *40*, 611. (c) Georghiou, P. E.; Tran, A. H.; Stroud, S. S.; Thompson, D. W. *Tetrahedron* **2006**, *62*, 2036.

(4) (a) Haino, T.; Yanase, M.; Fukazawa, Y. *Angew. Chem., Int. Ed.* **1997**, *36*, 259. (b) Haino, T.; Yanase, M.; Fukazawa, Y. *Angew. Chem., Int. Ed.* **1998**, *37*, 997. (c) Haino, T.; Yanase, M.; Fukunaga, C.; Fukazawa, Y. *Tetrahedron* **2006**, *62*, 2025.

(5) (a) Tsubaki, K.; Tanaka, K.; Kinoshita, T.; Fuji, K. *Chem. Commun.* **1998**, 895. (b) Ikeda, A.; Suzuki, Y.; Yoshimura, M.; Shinkai, S. *Tetrahedron* **1998**, *54*, 2497. (c) Mizyed, S.; Ashram, M.; Miller, D. O.; Georghiou, P. E. *J. Chem. Soc., Perkin Trans.* **2001**, *2*, 1916.

(6) (a) Andersson, T.; Nilsson, K.; Sundahl, M.; Westman, G.; Wennerström, O. *J. Chem. Soc., Chem. Commun.* **1992**, 604. (b) Yoshida, Z.-I.; Takekuma, H.; Takekuma, S.-I.; Matsubara, Y. *Angew. Chem., Int. Ed. Engl.* **1994**, *33*, 1597.

(7) Atwood, J. L.; Barnes, M. J.; Gardiner, M. G.; Raston, C. L. *Chem. Commun.* **1996**, 1449.

(8) Tribenzotriquinacenes: (a) Pham, D.; Bertran, J. C.; Olmstead, M. M.; Mascal, M.; Balch, A. L. *Org. Lett.* **2005**, *7*, 2805. (b) Georghiou, P. E.; Dawe, L. N.; Tran, H.-A.; Strübe, J.; Neumann, B.; Stammler, H.-G.; Kuck, D. *J. Org. Chem.* **2008**, *73*, 9040. (c) Bredenkçtter, B.; Henne, S.; Volkmer, D. *Chem.—Eur. J.* **2007**, *13*, 9931. Subphthalocyanines: (d) Claessens, C. G.; Torres, T. *Chem. Commun.* **2004**, 1298. (e) Shimizu, S.; Nakano, S.; Hosoya, T.; Kobayashi, N. *Chem. Commun.* **2011**, *47*, 316. (f) Sánchez-Molina, I.; Claessens, C. G.; Grimm, B.; Guldi, D. M.; Torres, T. *Chem. Sci.* **2013**, *4*, 1338. Anthracene-based hosts: (g) Kobayashi, J.; Domoto, Y.; Kawashima, T. *Chem. Lett.* **2010**, *39*, 134. (h) Kishi, N.; Li, Z.; Yoza, K.; Akita, M.; Yoshizawa, M. *J. Am. Chem. Soc.* **2011**, *133*, 11438. (i) Kishi, N.; Akita, M.; Kamiya, M.; Hayashi, S.; Hsu, H.-F.; Yoshizawa, M. *J. Am. Chem. Soc.* **2013**, *135*, 12976. Carbon nanorings: (j) Kawase, T.; Tanaka, K.; Fujiwara, N.; Darabi, H. R.; Oda, M. *Angew. Chem., Int. Ed.* **2003**, *42*, 1624. (k) Kawase, T.; Tanaka, K.; Seirai, Y.; Shiono, N.; Oda, M. *Angew. Chem., Int. Ed.* **2003**, *42*, 5597. (l) Kawase, T.; Fujiwara, N.; Tsutumi, M.; Oda, M.; Maeda, Y.; Wakahara, T.; Akasaka, T. *Angew. Chem., Int. Ed.* **2004**, *43*, 5060. (m) Iwamoto, T.; Watanabe, Y.; Sadahiro, T.; Haino, T.; Yamago, S. *Angew. Chem., Int. Ed.* **2011**, *50*, 8342. (n) Xia, J.; Bacon, J. W.; Jasti, R. *Chem. Sci.* **2012**, *3*, 3018. (o) Iwamoto, T.; Watanabe, Y.; Takaya, H.; Haino, T.; Yasuda, N.; Yamago, S. *Chem.—Eur. J.* **2013**, *19*, 14061. (p) Sato, S.; Yamasaki, T.; Isobe, H. *Proc. Natl. Acad. Sci. U.S.A.* **2014**, *111*, 8374. (q) Rahman, M. J.; Shimizu, H.; Araki, Y.; Ikeda, H.; Iyoda, M. *Chem. Commun.* **2013**, *49*, 9251. Porphyrin cages: (r) Tashiro, K.; Aida, T.; Zheng, J.-Y.; Kinbara, K.; Saigo, K.; Sakamoto, S.; Yamaguchi, K. J. *Am. Chem. Soc.* **1999**, *121*, 9477. (s) Sun, D.; Tham, F. S.; Reed, C. A.; Chaker, L.; Burgess, M.; Boyd, P. D. W. *J. Am. Chem. Soc.* **2000**, *122*, 10704. (t) Ayabe, M.; Ikeda, A.; Shinkai, S.; Sakamoto, S.; Yamaguchi, K. *Chem. Commun.* **2002**, 1032. (u) Shoji, Y.; Tashiro, K.; Aida, T. *J. Am. Chem. Soc.* **2006**, *128*, 10690. (v) Song, J.; Aratani, N.; Shinokubo, H.; Osuka, A. *J. Am. Chem. Soc.* **2010**, *132*, 16356. (w) Nakamura, T.; Ube, H.; Miyake, R.; Shionoya, M. *J. Am. Chem. Soc.* **2013**, *135*, 18790. Ex-TTF: (x) Pérez, E. M.; Sánchez, L.; Fernández, G.; Martin, N. *J. Am. Chem. Soc.* **2006**, *128*, 7172. (y) Huerta, E.; Isla, H.; Pérez, E. M.; Bo, C.; Martín, N.; de Mendoza, J. *J. Am. Chem. Soc.* **2010**, *132*, 5351. (z) Canevet, D.; Gallego, M.; Isla, H.; de Juan, A.; Pérez, E. M.; Martín, N. *J. Am. Chem. Soc.* **2011**, *133*, 3184.

(9) (a) Barth, W. E.; Lawton, R. G. J. *Am. Chem. Soc.* **1966**, *88*, 380. (b) Scott, L. T.; Hashemi, M. M.; Bratcher, M. S. *J. Am. Chem. Soc.* **1992**, *114*, 1920.

(10) Sakurai, H.; Daiko, T.; Hirao, T. *Science* **2003**, *301*, 1878.

(11) Dawe, L. N.; AlHujran, T. A.; Tran, H.-A.; Mercer, J. I.; Jackson, E. A.; Scott, L. T.; Georghiou, P. E. *Chem. Commun.* **2012**, *48*, 5563.

(12) This type of chirality has not been officially defined yet. Expanded Cahn−Ingold−Prelog rule was proposed by L. T. Scott et al. to designate the bowl-chirality. The *P* or *M* representation of the

bowl-type molecule **P2** was designated by their definition. See: Petrukhina, M.; Andreini, K. W.; Peng, L.; Scott, L. T. *Angew. Chem., Int. Ed.* **2004**, *43*, 5477.

(13) Examples of enantiopure molecules based on bowl-chirality: (a) Higashibayashi, S.; Sakurai, H. *J. Am. Chem. Soc.* **2008**, *130*, 8592. (b) Tan, Q.-T.; Higashibayashi, S.; Karanjit, S.; Sakurai, H. *Nature Commun.* **2012**, *3*, 891. (c) Shimizu, S.; Miura, A.; Khene, S.; Nyokong, T.; Kobayashi, N. *J. Am. Chem. Soc.* **2011**, *133*, 17322.

(14) Fullerene recognition by bowl-type molecular hosts: (a) Georghiou, P. E.; Tran, A. H.; Mizyed, S.; Bancu, M.; Scott, L. T. J. *Org. Chem.* **2005**, *70*, 6158. (b) Sygula, A.; Fronczek, F. R.; Sygula, R.; Rabideau, P. W.; Olmstead, M. M. J. *Am. Chem. Soc.* **2007**, *129*, 3842. (c) Constable, E. C.; Zhang, G.; Häussinger, D.; Housecroft, C. E.; Zampese, J. A. *J. Am. Chem. Soc.* **2011**, *133*, 10776.

(15) (a) Sasamori, T.; Tokitoh, N. In *Encyclopedia of Inorganic Chemistry*; King, R. B., Ed.; John Wiley: Chichester, 2005; p 1698. (b) Power, P. P. *Organometallics* **2007**, *26*, 4362.

(16) (a) Krebs, F. C.; Larsen, P. S.; Larsen, J.; Jacobsen, C. S.; Boutton, C.; Thorup, N. *J. Am. Chem. Soc.* **1997**, *119*, 1208. (b) Madsen, G. K. H.; Krebs, F. C.; Lebech, B.; Larsen, F. K. *Chem.—Eur. J.* **2000**, *6*, 1797.

(17) Nakai, Y.; Mori, T.; Inoue, Y. *J. Phys. Chem. A* **2012**, *116*, 7372.

(18) Hollas, J. M. *Modern Spectroscopy*, 4th ed.; John Wiley & Sons, Ltd.: New York, 2004; pp 73−102.

(19) Sakurai, H.; Tasaka, S.; Kira, M. J. *Am. Chem. Soc.* **1972**, *94*, 9285.

(20) (a) Suzuki, K.; Kobayashi, A.; Kaneko, S.; Takehira, K.; Yoshihara, T.; Ishida, H.; Shiina, Y.; Oishi, S.; Tobita, S. *Phys. Chem. Chem. Phys.* **2009**, *11*, 9850. (b) Ishida, H.; Tobita, S.; Hasegawa, Y.; Katoh, R.; Nozaki, K. *Coord. Chem. Rev.* **2010**, *254*, 2449.

(21) Berova, N.; Nakanishi, K.; Woody, R. W. *Circular dichroism: principles and applications*, 2nd ed.; Wiley-VCH: Weinheim, 2000.

(22) (a) Olmstead, M. M.; Costa, D. A.; Maitra, K.; Noll, B. C.; Phillips, S. L.; Van Calcar, P. M.; Balch, A. L. *J. Am. Chem. Soc.* **1999**, *121*, 7090. (b) Boyd, P. D. W.; Hodgson, M. C.; Rickard, C. E. F.; Oliver, A. G.; Chaker, L.; Brothers, P. J.; Bolskar, R. D.; Tham, F. S.; Reed, C. A. *J. Am. Chem. Soc.* **1999**, *121*, 10487.

(23) Fedurco, M.; Olmstead, M.; Fawcett, W. R. *Inorg. Chem.* **1995**, *34*, 390.

(24) (a) Welberry, T. R. In *Encyclopedia of Supramolecular Chemistry*; Atwood, J. T., Steed, J. W., Eds.; CRC Press: Boca Raton, FL, 2004; pp 457−466. (b) Rissanen, K. In *Encyclopedia of Supramolecular Chemistry*; Atwood, J. T., Steed, J. W., Eds.; CRC Press: Boca Raton, FL, 2004; pp 1586−1591.

(25) Fluorescence quenching, generally used method for fullerene recognition, was not applied to the system because the high-energy fluorescence of **P2** (λ_{flu} = 363 nm) was decreased by self-absorption of added C_{60}. It is difficult to distinguish the host−guest interaction with the self-absorption.

(26) (a) Blokzijl, W.; Engberts, J. B. F. N. *Angew. Chem., Int. Ed. Engl.* **1993**, *32*, 1545. (b) Schneider, H.-J. In *Encyclopedia of Supramolecular Chemistry*; Atwood, J. T., Steed, J. W., Eds.; CRC Press: Boca Raton, FL, 2004; pp 673−678.

(27) **G** was newly prepared by Prato reaction of C_{60} with PEGylated benzaldehyde, which was synthesized according to the literature. See: Xie, Y.; Akada, M.; Hill, J. P.; Ji, Q.; Charveta, R.; Ariga, K. *Chem. Commun.* **2011**, *47*, 2285.

(28) Akine, S. *TitrationFit*, program for analyses of host-guest complexation; Kanazawa University, Kanazawa, Japan, 2013.

(29) (a) Marconi, G.; Mayer, B.; Klein, Ch. Th.; Köhler, G. *Chem. Phys. Lett.* **1996**, *260*, 589. (b) Liu, Y.; Liang, P.; Chen, Y.; Zhao, Y.-L.; Ding, F.; Yu, A. *J. Phys. Chem. B* **2005**, *109*, 23739. (c) Dan Pantos, G.; Wietor, J.-L.; Sanders, J. K. M. *Angew. Chem., Int. Ed.* **2007**, *46*, 2238. (d) Sokolov, V. I.; Bashilov, V. V.; Dolgushin, F. M.; Abramova, N. V.; Babievsky, K. K.; Ginzburg, A. G.; Petrovskii, P. V. *Tetrahedron Lett.* **2009**, *50*, 5347.

(30) There have been many reports of chiral fullerens connected with chiroptical units via covalent bonds. See: Thilgen, C.; Diederich, F. *Chem. Rev.* **2006**, *106*, 5049.

(31) Shoji, Y.; Tashiro, K.; Aida, T. *J. Am. Chem. Soc.* **2010**, *132*, 5928.

(32) Burla, M. C.; Caliandro, R.; Camalli, M.; Carrozzini, B.; Cascarano, G. L.; De Caro, L.; Giacovazzo, C.; Polidori, G.; Spagna, R. *J. Appl. Crystallogr.* **2005**, *38*, 381.

(33) (a) Sheldrick, G. M. *SHELX97*, Program for crystal structure determination; Universität Göttingen, Göttingen, Germany, 1997. (b) *SHELX2014*, Program for crystal structure determination; Universität Göttingen, Göttingen, Germany, 2014.

(34) Frisch, M. J.; et al. *Gaussian 09*, Revision A.02; Gaussian, Inc.: Wallingford, CT, 2009.

(35) Zhao, Y.; Truhlar, D. G. *Theor. Chem. Acc.* **2008**, *120*, 215.